Human cytomegalovirus glycoprotein B variants affect viral entry, cell fusion, and genome stability

Jiajia Tang[a], Giada Frascaroli[a], Robert J. Lebbink[b], Eleonore Ostermann[a], and Wolfram Brune[a,1]

[a]Heinrich Pette Institute, Leibniz Institute for Experimental Virology, 20251 Hamburg, Germany; and [b]Medical Microbiology, University Medical Center Utrecht, 3584CX Utrecht, Netherlands

Edited by Thomas E. Shenk, Princeton University, Princeton, NJ, and approved July 23, 2019 (received for review April 30, 2019)

Human cytomegalovirus (HCMV), like many other DNA viruses, can cause genome instability and activate a DNA damage response (DDR). Activation of ataxia-telangiectasia mutated (ATM), a kinase activated by DNA breaks, is a hallmark of the HCMV-induced DDR. Here we investigated the activation of caspase-2, an initiator caspase activated in response to DNA damage and supernumerary centrosomes. Of 7 HCMV strains tested, only strain AD169 activated caspase-2 in infected fibroblasts. Treatment with an ATM inhibitor or inactivation of PIDD or RAIDD inhibited caspase-2 activation, indicating that caspase-2 was activated by the PIDDosome. A set of chimeric HCMV strains was used to identify the genetic basis of this phenotype. Surprisingly, we found a single nucleotide polymorphism within the AD169 UL55 ORF, resulting in a D275Y amino acid exchange within glycoprotein B (gB), to be responsible for caspase-2 activation. As gB is an envelope glycoprotein required for fusion with host cell membranes, we tested whether gB(275Y) altered viral entry into fibroblasts. While entry of AD169 expressing gB(275D) proceeded slowly and could be blocked by a macropinocytosis inhibitor, entry of wild-type AD169 expressing gB(275Y) proceeded more rapidly, presumably by envelope fusion with the plasma membrane. Moreover, gB(275Y) caused the formation of syncytia with numerous centrosomes, suggesting that cell fusion triggered caspase-2 activation. These results suggest that gB variants with increased fusogenicity accelerate viral entry, cause cell fusion, and thereby compromise genome stability. They further suggest the ATM-PIDDosome-caspase-2 signaling axis alerts the cell of potentially dangerous cell fusion.

cytomegalovirus | DNA damage response | caspase-2 | syncytium

Human cytomegalovirus (HCMV, human herpesvirus 5) is an opportunistic pathogen that is highly prevalent in human populations worldwide. It causes mild infections in otherwise healthy individuals, but is a leading cause for morbidity and mortality in immunocompromised transplant patients. Moreover, it is the most frequent cause for congenital infections (1). HCMV has also been detected in brain tumors (2). However, its role in oncogenesis or oncomodulation has remained controversial (3).

HCMV replicates its large double-stranded DNA genome in the host cell nucleus (1). It stimulates quiescent cells to enter the cell cycle and subsequently arrests the cell cycle at the G1/S transition in order to create optimal conditions for viral DNA replication while preventing cellular DNA replication (4, 5). However, when a cell is infected after DNA replication has started, viral immediate-early (IE) gene expression is suppressed and the cell divides before arresting in the next cycle. This regulation serves to prevent mitosis during ongoing viral replication, which can lead to mitotic catastrophe and cell death (6).

Entry of the viral linear DNA genome and its replication and processing in the host cell nucleus activates a DNA damage response (DDR) (7). It is initiated primarily by the protein kinases ATM (ataxia-teleangiectasia mutated) and ATR (ATM and RAD3-related), which serve as sensors for double- and single-stranded DNA breaks, respectively (8–10). They activate downstream substrates such as p53 and checkpoint proteins to arrest the cell cycle, activate DNA repair, and prevent replication of damaged DNA (11). When DNA damage is too severe, programmed cell death is initiated to eliminate the damaged cell, thereby maintaining genome stability (11).

Viral manipulation of the cell cycle and activation of the DDR result in stress and can trigger apoptosis, the most common form of programmed cell death. Initiation and execution of apoptosis is governed by caspases, a family of conserved cysteine-dependent aspartate-specific proteases. HCMV inhibits apoptosis by expressing several apoptosis suppressors (12). These include the viral mitochondrion-localized inhibitor of apoptosis (vMIA), which suppresses apoptosis induction by intrinsic stress stimuli (13), and the viral inhibitor of caspase-8 activation (vICA), which blocks the extrinsic, death receptor-dependent apoptosis pathway (14).

Caspase-2 is one of the evolutionarily most conserved caspases, yet its function has remained enigmatic for a long time (15). More recently, accumulating evidence indicated an important role of caspase-2 in the maintenance of genomic stability (16). Caspase-2 can be activated by DNA damage, cell cycle dysregulation, and abnormal mitosis. Its activation requires proximity-induced dimerization and autocatalytic cleavage. The best characterized activation platform is the PIDDosome, which consists of PIDD (p53-induced protein with a death domain), RAIDD (RIP-associated ICH-1 homologous protein with a death domain), and caspase-2 (17). PIDDosome assembly requires ATM-mediated phosphorylation of PIDD (18).

Significance

Human cytomegalovirus (HCMV) is a major cause of morbidity and mortality in transplant patients and the most common infectious cause of birth defects. Although HCMV is not a generally accepted cause of cancer, it shares similarities to cancer-causing viruses: It dysregulates the cell cycle, activates the DNA damage response, and suppresses apoptosis. However, causes and consequences of these viral properties remain poorly understood. Here we show that HCMV activates caspase-2, an apoptosis-related enzyme activated by DNA damage and abnormal mitosis, in a strain-specific manner. Caspase-2 activation depends on envelope glycoprotein B variants with increased fusogenicity, which facilitate viral entry, promote cell fusion, and affect genome stability. These results suggest that specific glycoprotein B variants might affect HCMV transmission and pathogenicity.

Author contributions: J.T. and W.B. designed research; J.T., G.F., and E.O. performed research; R.J.L. contributed new reagents/analytic tools; J.T., G.F., E.O., and W.B. analyzed data; and J.T. and W.B. wrote the paper.

The authors declare no conflict of interest.

This article is a PNAS Direct Submission.

[1]To whom correspondence may be addressed. Email: wolfram.brune@leibniz-hpi.de.

This article contains supporting information online at www.pnas.org/lookup/suppl/doi:10.1073/pnas.1907447116/-/DCSupplemental.

Published online August 19, 2019.

Most studies on caspase-2 have focused on its role in cancer and apoptosis, and little is known about its role in infection. As HCMV can activate the DDR (7), manipulate the cell cycle (4, 5), and cause abnormal mitosis (19, 20), we decided to investigate whether caspase-2 is activated during the course of HCMV infection. We found that HCMV strain AD169 activates caspase-2 through the ATM-PIDDosome signaling pathway, while 6 other strains do not activate caspase-2. Unexpectedly, the cause of this phenotype does not reside in a DDR or cell cycle-related gene, but in the viral *UL55* gene. *UL55* encodes glycoprotein B (gB), a viral envelope glycoprotein essential for viral infection. It mediates fusion of the viral envelope with host cell membranes (21). We show that the AD169 gB(275Y) variant mediates rapid viral entry, induces the formation of syncytia with numerous centrosomes, and activates caspase-2. We further show that the gB(585G) variant of strain VR1814 also induces cell fusion and caspase-2 activation. These results suggest that gB variants with increased fusogenicity affect viral entry, cell fusion, and genome stability.

Results

HCMV Activates Caspase-2 in a Strain-Specific Manner. HCMV induces a DDR involving activation of the protein kinase ATM (7–10). As ATM activation can promote caspase-2 activation during the DDR (18), we investigated whether HCMV infection activates caspase-2. To do this, we infected human embryonic lung fibroblasts (MRC-5 cells) with HCMV and analyzed caspase-2 activation by immunoblot detection of the active p19 cleavage product, the most commonly used detection method for caspase-2 activation. Upon infection with the HCMV laboratory strain AD169, increasing amounts of p19 were detected starting 9 h postinfection (hpi) (Fig. 1*A*). To test whether HCMV generally activates caspase-2, we did the same experiment with 2 other HCMV strains, TB40/E and TR. However, caspase-2 activation was minimal or absent in MRC-5 cells infected with these strains (Fig. 1 *B* and *C*). We also tested 4 additional HCMV strains (Towne, Toledo, PH, and FIX), but none of them activated caspase-2 as AD169 did (summarized in Fig. 1*D*). Thus, we concluded that caspase-2 activation by HCMV is strain-specific.

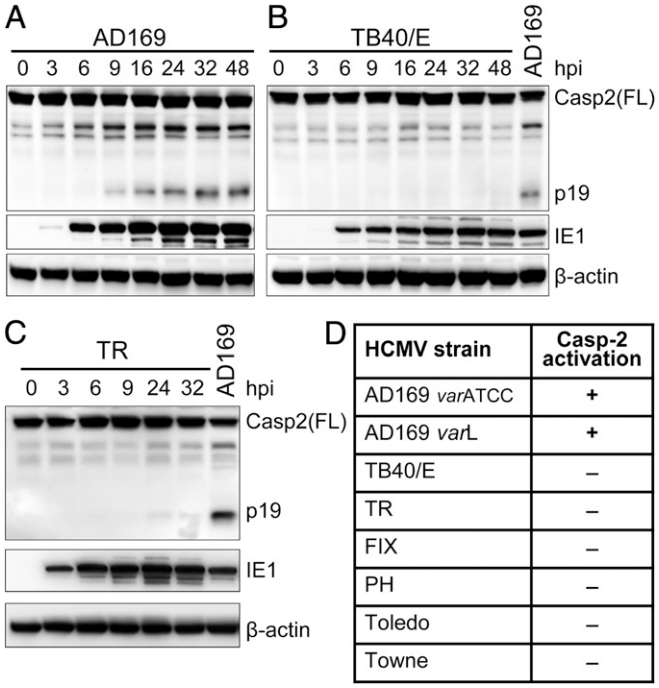

D

HCMV strain	Casp-2 activation
AD169 *var*ATCC	+
AD169 *var*L	+
TB40/E	–
TR	–
FIX	–
PH	–
Toledo	–
Towne	–

Fig. 1. HCMV activates caspase-2 in a strain-specific manner. MRC-5 fibroblasts were infected with HCMV strains AD169 (*A*), TB40/E (*B*), and TR (*C*) at MOI 5. Cells were harvested at the indicated times postinfection and caspase-2 activation was analyzed by immunoblot using an antibody recognizing the caspase-2 p19 subunit. IE1 and β-actin were used as infection and loading controls, respectively. (*D*) Table summarizing caspase-2 activation by different HCMV strains. Two variants (ATCC and Long) of AD169 were tested.

Caspase-2 Activation by AD169 Is Cell Cycle-Dependent. It has been shown in several experimental models that caspase-2 activation occurs when genetically damaged cells pass through mitosis (22–24). To test whether HCMV-induced caspase-2 activation requires transition through mitosis, we treated infected cells with inhibitors of mitotic entry (RO-3306) or mitotic exit (nocodazole). Indeed, treatment with these inhibitors prevented caspase-2 activation (Fig. 2*A*).

It is well established that HCMV arrests the cell cycle at the G1/S transition. However, when cells are infected at later stages of the cell cycle, they pass through mitosis before the G1/S block is installed in the following cycle (25, 26). As the previous experiments were done with asynchronous cells, we wanted to test whether the cell cycle state at the time of infection determines caspase-2 activation. To do this, we synchronized cells by serum starvation and infected them at defined times after release from the starvation-induced cell cycle arrest (Fig. 2*B*). As an indicator of the cell cycle state, cellular DNA content was measured by flow cytometry (Fig. 2*C*). As shown in Fig. 2*D*, caspase-2 was not activated in cells infected in G0 or early G1, whereas a strong activation was detected when cells were infected in late G1. Taken together, these data suggested that caspase-2 activation occurs when AD169 cannot arrest the cell cycle and infected cells pass through mitosis.

AD169-Induced Caspase-2 Activation Requires ATM and the PIDDosome. Although caspase-2 has been classified as an initiator caspase, it can also be cleaved by other caspases, such as caspase-3 and caspase-8 (27). Since HCMV strain AD169 carries an inactivating mutation in the UL36-encoded viral inhibitor of caspase-8 activation (14), we tested whether caspase-2 activation in AD169-infected cells occurs downstream of caspase-8. To do this, we treated cells with the caspase-8 inhibitor, Z-IETD-FMK. However, even high concentrations of Z-IETD-FMK did not reduce caspase-2 cleavage (*SI Appendix*, Fig. S1). Treatment of uninfected cells with TNF-α and cycloheximide induced activation of caspase-8 and caspase-3, and this was inhibited by Z-IETD-FMK. However, even TNF-α treatment did not result in caspase-2 activation (i.e., appearance of caspase-2 p19), but only induced an increased abundance of the p33 fragment (*SI Appendix*, Fig. S1). From these results we concluded that caspase-2 activation was independent of caspase-8.

The PIDDosome is a platform for caspase-2 activation in response to DNA damage (17, 23) (Fig. 3*A*). In order to test whether caspase-2 is activated by the PIDDosome in AD169-infected cells, we used CRISPR/Cas9 gene editing to inactivate PIDD and RAIDD in telomerase-immortalized human foreskin fibroblasts (HFF). Indeed, caspase-2 p19 was not detected in PIDD- or RAIDD-deficient HFF upon infection (Fig. 3*B*), indicating that caspase-2 is activated via the PIDDosome.

ATM can trigger PIDDosome assembly by phosphorylating PIDD, thereby promoting its interaction with RAIDD (18) (Fig. 3*A*). Since HCMV infection is known to activate ATM (8, 10), we tested whether ATM was involved in caspase-2 activation by AD169. When infected fibroblasts were treated with increasing concentrations of the ATM inhibitor KU-60019, the abundance of p19 decreased in a concentration-dependent manner (Fig. 3*C*). Moreover, caspase-2 activation was not detected in infected ATM-deficient fibroblasts (Fig. 3*D*). These results suggested that

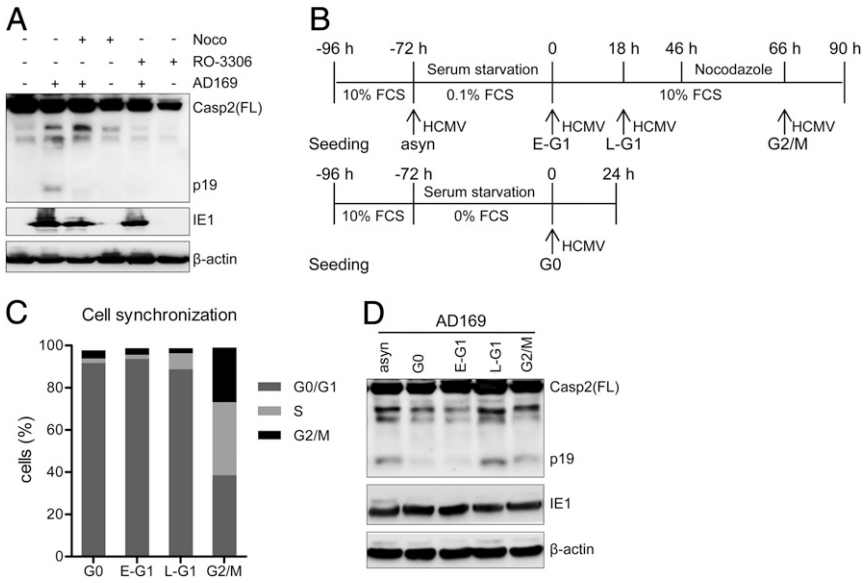

Fig. 2. Caspase-2 activation by AD169 is cell cycle-dependent. (*A*) MRC-5 fibroblasts were pretreated with a mitotic entry inhibitor (RO-3306, 10 μM) or a mitotic exit inhibitor (nocodazole, 0.66 μM) for 1 h. Cells were infected with HCMV AD169 (MOI 5) and collected at 24 hpi. Caspase-2 activation was analyzed by immunoblot. IE1 and β-actin were used as infection and loading controls, respectively. (*B*) MRC-5 fibroblasts were seeded and synchronized according to a previously described protocol (77) with a few modifications. Asynchronous (asyn) cells were infected before serum starvation. Synchronized cells were infected in G0, early G1 (E-G1), late G1(L-G1), or G2/M phase. (*C*) Synchronized cells were collected, fixed with ethanol, stained with propidium iodide (PI), and analyzed by flow cytometry. (*D*) Synchronized cells infected with HCMV AD169 for 24 h were analyzed for caspase-2 activation by immunoblot. The data shown in this figure are representative of 2 independent experiments.

caspase-2 activation by HCMV AD169 infection involves ATM activation and PIDDosome assembly.

An AD169-specific gB Variant Is Responsible for Caspase-2 Activation. Previous studies have shown that HCMV infection triggers a DDR involving activation of ATM (8–10). However, we only observed caspase-2 activation by AD169 but not by 6 other strains (Fig. 1), suggesting that DDR and ATM signaling are not sufficient to activate caspase-2. Hence it was reasonable to assume that AD169 either expresses a unique gene product or variant that triggers caspase-2 activation or lacks an inhibitor of caspase-2 activation, which is present in the other strains. HCMV strains show a substantial genomic variability with a high number of single-nucleotide polymorphisms (SNPs) across the viral genome, many of which are coding relevant and thus affect the amino acid composition of viral proteins (28, 29). In order to identify which viral gene is responsible for this phenotype, we compared the coding sequences of all 7 strains and found that around 120 gene products of AD169 contain amino acid residues not shared by the other 6 strains. Among those, we focused on 7 genes as most promising candidates based on their involvement in DDR, cell cycle, or cell death regulation: *UL32*, *UL36*, *UL69*, *UL76*, *UL82*, *UL97*, and *UL117* (*SI Appendix*, Fig. S2*A*). The first candidate we tested was *UL76*, which is known to activate the DDR (30). We found that *UL76* contains 4 AD169-specific amino acid residues and hypothesized that they might contribute to caspase-2 activation. Thus we exchanged them between AD169 and strain TB40/E by bacterial artificial chromosome (BAC) mutagenesis. However, they were not responsible for caspase-2 activation (*SI Appendix*, Fig. S2 *B* and *C*). In a similar way, we also tested the other 6 candidate genes. Much to our chagrin, none of the AD169-specific amino acid variants were responsible for caspase-2 activation.

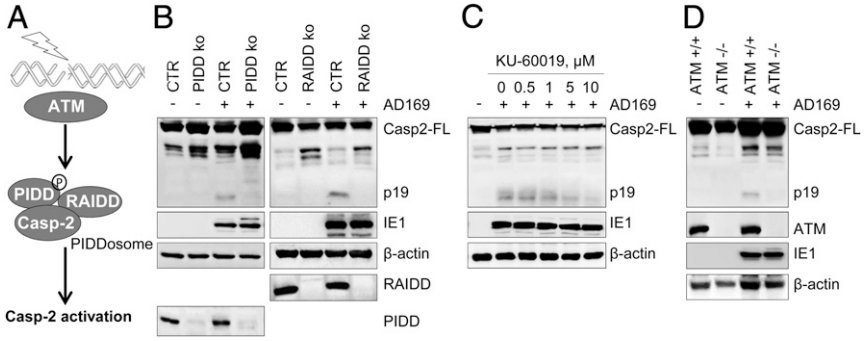

Fig. 3. AD169-induced caspase-2 activation requires ATM and the PIDDosome. (*A*) ATM-PIDDosome signaling pathway of caspase-2 activation. (*B*) PIDD or RAIDD knockout and control (CTR) HFF were infected with HCMV AD169. Samples were collected 24 hpi and caspase-2 activation was analyzed using immunoblot analysis. (*C*) MRC-5 cells were pretreated with ATM inhibitor (KU-60019) for 1 h at indicated concentration, then infected by AD169. (*D*) ATM-deficient dermal fibroblasts and control cells were infected with AD169 and caspase-2 activation was analyzed. The data shown in this figure are representative of 3 independent experiments.

As the candidate gene approach had been unsuccessful, we decided to narrow down the responsible genomic region by constructing chimeric strains consisting of AD169 and TB40/E as recently described (31) and shown in Fig. 4*A*. Using this "copy & paste" strategy, we consecutively transferred 15-kbp fragments of TB40/E to AD169 and tested each chimeric virus for its ability to activate caspase-2. After exchange of 3 fragments (A: *UL112-UL127*; B: *UL69-UL77*; C: *UL48A-UL55*), AD169:ABC had lost the ability to activate caspase-2 (Fig. 4*B*). This result indicated that the gene responsible for the caspase-2 phenotype resides in the fragment C. This fragment encodes 8 genes (*UL48A-UL55*) (Fig. 4*C*), all of which are essential for viral replication (32). *UL48A*, *UL50*, *UL51*, and *UL53* do not contain AD169-specific amino acid residues. *UL52* was excluded as it is expressed with late kinetics and is not a virion protein (33), making it an unlikely cause of a phenotype occurring as early as 9 hpi (Fig. 1*A*). Of the remaining 3 genes (*UL49*, *UL54*, and *UL55*) we decided to first test *UL55*, which encodes the viral gB. AD169 gB contains a tyrosine (Y) residue at amino acid position 275, where the other strains encode an aspartic acid (D) residue (Fig. 4*D*). To test whether this gB variant is the responsible factor, we changed Y to D at position 275 by BAC mutagenesis. Indeed, the AD169 gB(275D) mutant did not activate caspase-2 (Fig. 4*E*). Conversely, a gB(275Y) mutant of strain TB40/E gained the ability to activate caspase-2 (Fig. 4*E*), further confirming that gB is responsible for the observed phenotype.

AD169 gB(275Y) Induces Cell Fusion and Supernumerary Centrosomes. HCMV gB mediates viral entry through fusion of the viral envelope with cellular membranes in cooperation with other glycoproteins, such as gH and gL (21, 34–36). It has also been shown that overexpression of gB can promote syncytium formation in U373 glioblastoma cells, suggesting that gB can also promote cell fusion (37). Thus, we wondered whether an increased fusogenicity of gB(275Y) could be the cause of caspase-2 activation.

Recent studies have reported that cytokinesis failure activates caspase-2 (23) and that caspase-2 functions as a sensor of supernumerary centrosomes and participates in the elimination of aneuploid and polyploid cells (23, 24). Since cytokinesis failure and cell fusion should both lead to supernumerary centrosomes, we tested whether AD169 causes increased cell fusion. For this purpose, we designed a system that allows us to detect fused cells. We first transduced fibroblasts with retroviral vectors expressing either EGFP or mCherry and mixed equal numbers of green and red cells. Then we infected the cells with wild-type and mutant variants of AD169 and TB40/E. While fused cells should exhibit green and red fluorescence, nonfused cells should be either green or red (Fig. 5*A*). Infection of fibroblasts with gB(275Y) variants of AD169 and TB40/E induced the formation of numerous syncytia with multiple nuclei, whereas syncytium formation was infrequent after infection with gB(275D) variants (Fig. 5 *B* and *C*). Consequently, we detected multiple centrosomes in these syncytia by γ-tubulin staining (Fig. 5*D*).

When a cell with 2 or more nuclei and more than 2 centrosomes enters mitosis, the process can become aberrant, leading to mitotic catastrophe and cell death (38). Indeed, aberrant mitotic figures have previously been observed in up to 30% of AD169-infected cells, but only infrequently in cells infected with strains Towne or TB40/E (19, 20). Moreover, inactivation of the viral mitochondrial inhibitor of apoptosis (vMIA, encoded by ORF UL37x1) in AD169 resulted in apoptosis of infected cells (39), whereas inactivation of vMIA in Towne did not (40). Based on these published observations, we tested whether the gB(275Y) variant of AD169 was also responsible for the proapoptotic trait of AD169. To exclude a role of UL36/vICA (which is inactive in AD169), we first repaired the *UL36* mutation in both gB variants of AD169. Subsequently, UL37x1/vMIA was deleted from the 2 viral genomes. Consistent with previous observations (39), deletion of *UL37x1* substantially reduced the viability of cells infected with AD169 gB(275Y)

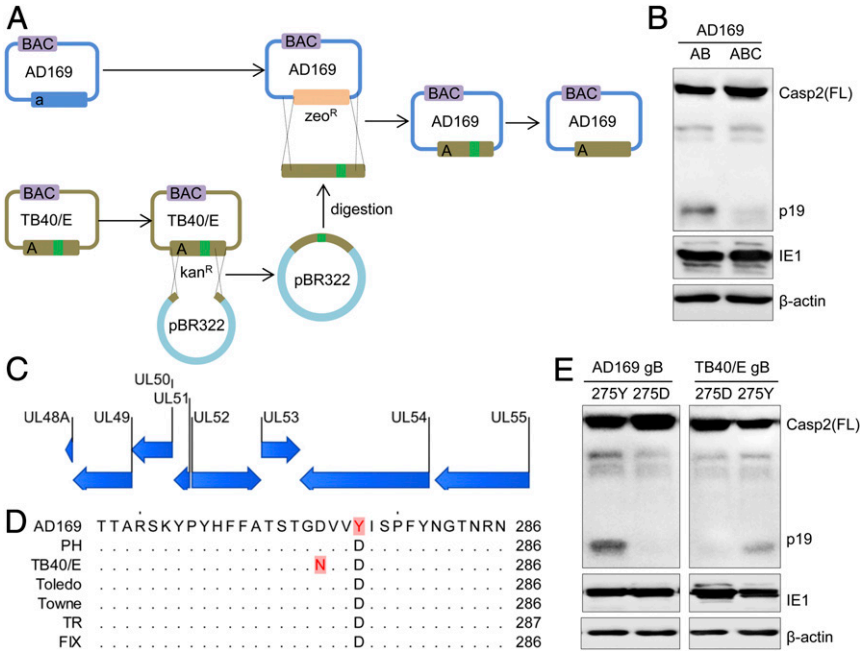

Fig. 4. An AD169-specific variant of gB is responsible for caspase-2 activation. (*A*) Construction of chimeric virus genomes by copy-paste mutagenesis (31). (*B*) Caspase-2 activation by chimeric virus AD169:AB but not by AD169:ABC. (*C*) Gene content of fragment C. (*D*) Sequence alignment of UL55-encoded gB shows an AD169-specific 275Y variant. (*E*) Amino acid 275 was changed from Y to D in AD169 and from D to Y in TB40/E. Caspase-2 activation by AD169 and TB40/E gB variants was analyzed by immunoblot. The data shown are representative of 3 (*B*) or 2 (*E*) independent experiments.

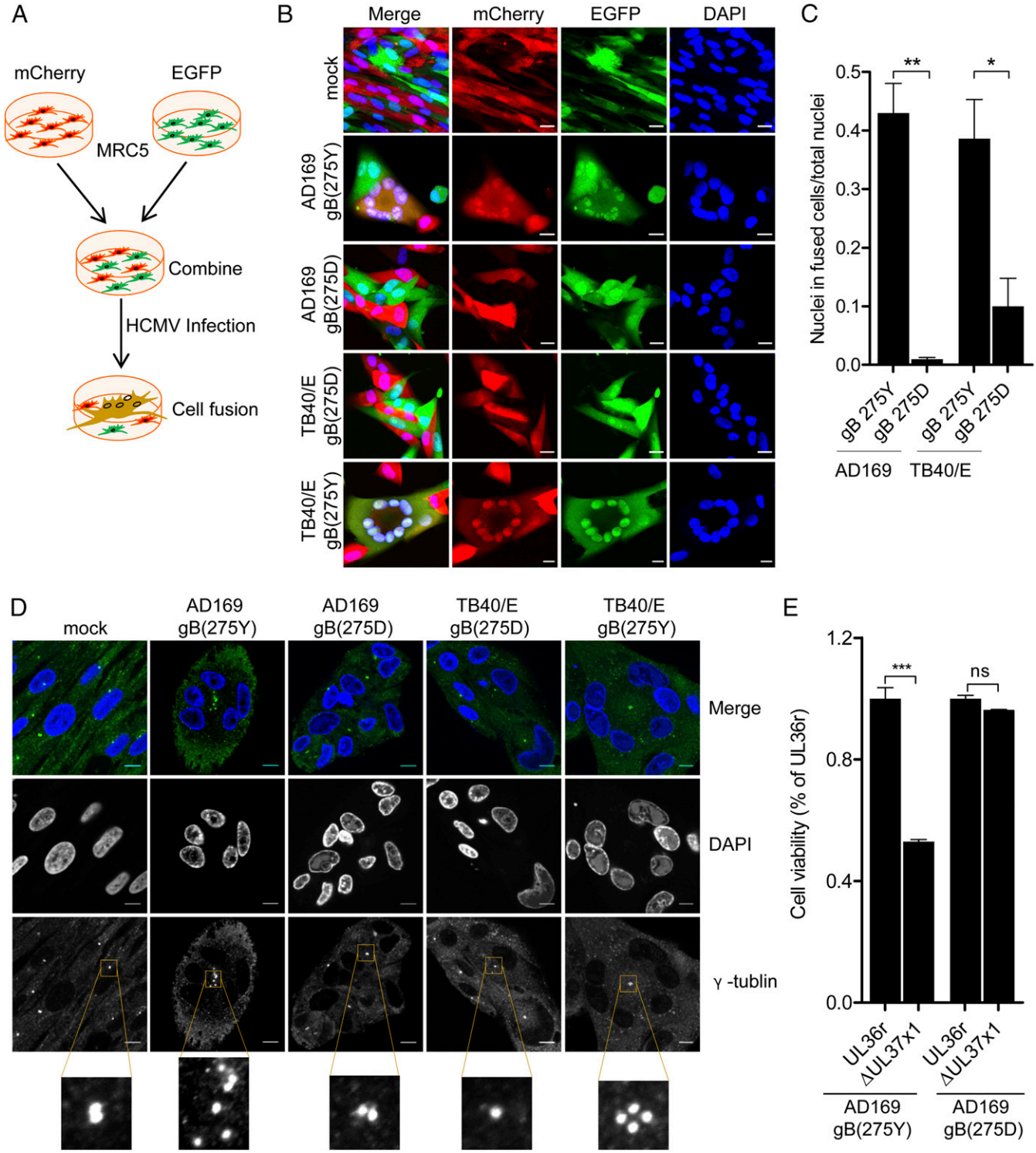

Fig. 5. gB(275Y) promotes cell fusion, supernumerary centrosomes, and cell death. (*A*) Experimental design for the detection of HCMV-induced cell fusion. (*B*) MRC-5 cells were transduced with retroviral vectors expressing EGPF or mCherry, mixed equally, then infected with HCMV (MOI 5). Cells were fixed at 48 hpi and nuclei were stained with DAPI. (Scale bars, 20 μm.) (*C*) To quantifiy cell fusion, 3 individual experiments were performed and ≥500 nuclei were counted for each experiment. Means ± SEM are shown. (*D*) MRC-5 cells were infected as above, fixed at 48 hpi, and stained with an antibody against γ-tublin to identify centrosomes and DAPI for nuclei. (Scale bars, 10 μm.) (*E*) The AD169 *UL36* mutation was repaired (UL36r) and then *UL37x1* was deleted. MRC-5 cells were infected with 2 sets of viruses: gB(275Y) and gB(275D). Cell viability was derterminded 5 dpi by using an ATP assay and normalized to the corresponding parental (UL36r) virus. Means ± SEM ($n = 3$) are shown. Significance was determined by 1-way ANOVA with Tukey's multiple comparison post test. *$P < 0.05$; **$P < 0.01$; ***$P < 0.001$; ns, not significant.

(Fig. 5*E*). This phenotype was absent in AD169 gB(275D), suggesting that the gB(275Y) variant is responsible for the proapoptotic phenotype.

The gB(275Y) Variant Accelerates Viral Entry. Since gB plays an essential role in viral entry (21), we tested whether the 2 gB variants affect the kinetics of viral gene expression. MRC-5 fibroblasts

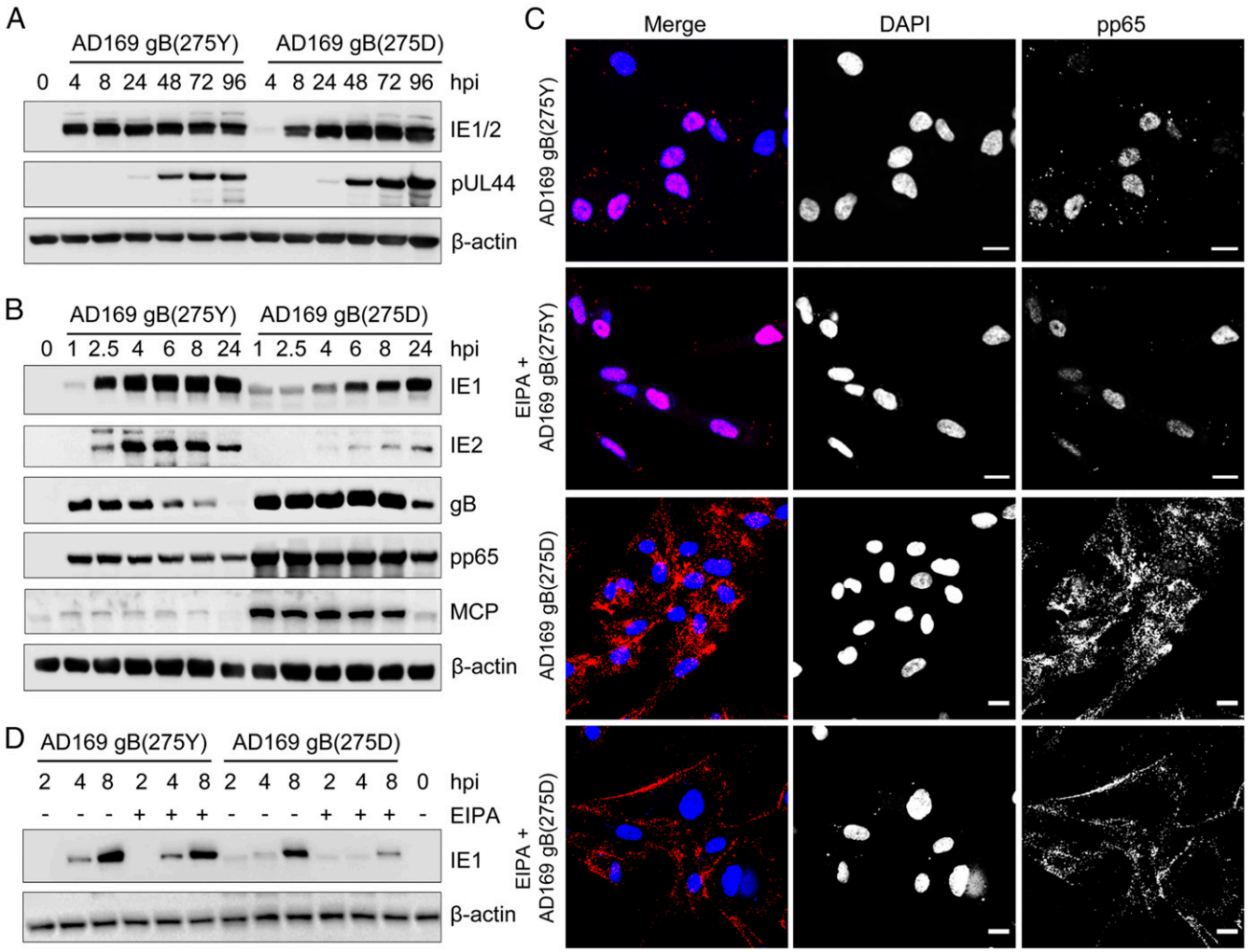

Fig. 6. The gB(275Y) variant accelerates viral entry. (*A* and *B*) MRC-5 fibroblasts were infected by AD169 gB(275Y) or gB(275D) (MOI 3) and harvested at the indicated times postinfection. Viral protein levels were determined by immunoblot analysis; β-actin was used as a loading control. (*C*) MRC-5 fibroblasts were pretreated for 30 min with 100 μM EIPA or vehicle. Two hours postinfection with AD169 gB variants (MOI 3), cells were fixed and the viral tegument protein pp65 was detected by indirect immunofluorescence. Nuclei were stained with DAPI. (Scale bars, 20 μm.) Images representative of 3 independent experiments are shown. (*D*) MRC-5 cells were pretreated and infected as above. Two hours postinfection EIPA was removed and fresh medium was added. Cells were harvested at the indicated times and IE1 expression was analyzed by immunoblot. The data shown are representative of 3 independent experiments.

were infected with gB(275Y) and gB(275D) variants of AD169, and the expression of the IE proteins 1 and 2 (IE1/2) and the early protein pUL44 was detected by immunoblot analysis. While pUL44 expression was similar for both variants, IE1/2 expression appeared to be delayed in cells infected with the gB(275D) variant (Fig. 6*A* and *SI Appendix*, Fig. S4 *C* and *D*). This finding was confirmed in a subsequent experiment using IE1- and IE2-specific antibodies and more time points within the first 8 hpi (Fig. 6*B*). Immediately after infection, we detected larger amounts of the viral tegument protein pp65, the envelope gB, and major capsid protein (MCP) in cells infected with AD169 gB(275D) (Fig. 6*B*), suggesting that AD169 gB(275D) is less infectious than AD169 gB(275Y). To verify this hypothesis, we determined the replication kinetics of both AD169 variants. Infectious virus release was measured by titration (*SI Appendix*, Fig. S3*A*), and viral genome copy numbers were quantified by quantitative real-time PCR (*SI Appendix*, Fig. S3*B*). Indeed, while the release of viral particles (measured as genome copies) was similar for both viruses, viral titers were generally lower, resulting in a 4- to 40-fold lower infectivity of AD169 gB(275D) compared to AD169 (*SI Appendix*, Fig. S3*B*). We also determined the ratio of genomes to infectious units (IU) of 4 stock preparations for each virus. Again, the genome/IU ratios were higher for the gB(275D) virus as compared to the gB(275Y) virus (*SI Appendix*, Fig. S3*C*). Collectively, these data suggested that AD169 gB(275D) is less infectious.

Next we wanted to determine whether the delayed IE1/2 expression was caused by a delayed virus entry. HCMV is thought to enter fibroblasts either by fusion of the viral envelope with the plasma membrane (41, 42) or by macropinocytosis (43). Fusion with the plasma membrane results in a rapid release of the viral tegument protein pp65 into the cytosol and rapid translocation of pp65 to the nucleus within the first 2 h. In contrast, HCMV infection of epithelial and endothelial cells occurs by endocytosis (macropinocytosis) of viral particles, delayed fusion of the viral envelope with the endosomal membrane, and delayed nuclear accumulation of pp65 (44–46). When we infected fibroblasts with the 2 AD169 gB variants and determined the localization of pp65 by immunofluorescence, we found that pp65 of AD169 gB(275Y) was predominantly nuclear at 2 hpi. In contrast, pp65 of AD169 gB(275D) was predominantly in cytoplasmic dots at 2 hpi and accumulated in the nucleus with delay (Fig. 6*C* and *SI Appendix*, Fig. S4 *A* and *B*). Addition of the macropinocytosis

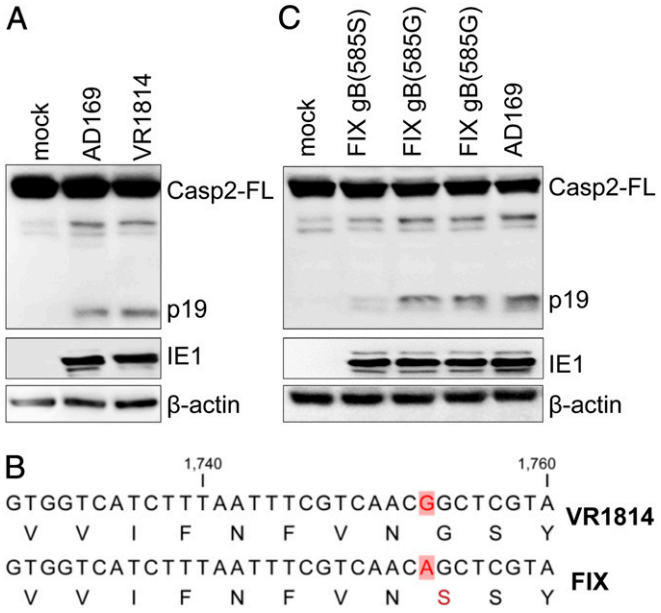

Fig. 7. VR1814 gB(585G) can also activate caspase-2. (*A*) Caspase-2 was activated upon infection of MRC-5 cells with HCMV strain VR1814. (*B*) *UL55* sequence alignment of FIX and VR1814. (*C*) FIX gB(585S) was changed to 585G by BAC mutagenesis (2 clones are shown). Caspase-2 activation was analyzed by immunoblot. The data shown are representative of 3 (*A*) or 2 (*B*) independent experiments.

inhibitor ethyl-isopropyl amiloride (EIPA) inhibited entry (Fig. 6*C*) and IE1 expression (Fig. 6*D*) of AD169 gB(275D), but did not affect AD169 gB(275Y). These data suggested that gB(275Y) facilitates rapid entry, probably by fusion with the plasma membrane, whereas gB(275D) allows delayed entry by a pathway that can be inhibited by EIPA.

Caspase-2 Activation Is Not a Unique Property of AD169. In order to determine whether the more fusogenic gB(275Y) variant is a unique property of strain AD169, we screened all HCMV gB sequences available at GenBank for the presence of the 275Y variant. It was present in all sequenced variants of strain AD169 (varATCC, varUK, varUC, and varL) and in strain N12 (GenBank accession no. CAA07368), suggesting that this gB variant is rare but not unique to AD169. However, we hypothesized that other highly fusogenic gB variants exist, which could elicit similar phenotypes as gB(275Y) does. For example, the clinical isolate VR1814 has been reported to induce syncytia upon infection of epithelial cells (47). Thus we tested whether VR1814 infection activates caspase-2. Indeed, caspase-2 was activated in MRC-5 cells upon infection with VR1814 (Fig. 7*A*). This finding was unexpected as infection with strain FIX [a BAC clone of VR1814 (48)] did not activate caspase-2 (Fig. 1*D*). However, FIX is known to differ in a limited number of nucleotides from VR1814 (49), and our sequence analysis of gB revealed a SNP resulting in gB(585G) in VR1814 vs. gB(585S) in FIX (Fig. 7*B*). To test whether this gB polymorphism was responsible for syncytium formation and caspase-2 activation, we changed gB(585S) to (585G) by mutagenesis of the FIX BAC. Indeed, this change was sufficient to induce syncytium formation (*SI Appendix*, Fig. S5) and caspase-2 activation (Fig. 7*C*) by FIX gB(585G). These results suggested that gB(585G) has a similar effect on cell fusion as gB(275Y) does.

Discussion

In this study we show that HCMV strain AD169 triggers cell fusion resulting in supernumerary centrosomes and activation of caspase-2 via the PIDDosome. Caspase-2 activation was prevented by mitosis inhibitors (Fig. 2*A*), indicating that infected cells passed through mitosis. In synchronized cells, caspase-2 activation occurred when cells were infected in late G1 (Fig. 2*D*), suggesting that the virus was unable to install a cell cycle arrest at the G1/S transition in these cells. Consequently, the infected and fused cells could undergo mitosis with potentially deleterious consequences, such as aberrant mitosis, aneuploidy, and mitotic catastrophe. Apoptosis, a frequent consequence of failed mitosis, was suppressed by the viral apoptosis inhibitor vMIA (Fig. 5*E*). Hence, HCMV-induced cell fusion can lead to genome instability. Our data further suggest that the ATM-PIDDosome-Caspase-2 signaling axis serves to alert the cell of potentially dangerous fusions of mitotically active cells.

In hindsight, this study provides a mechanistic explanation for several previously observed properties of HCMV strain AD169: The ability to induce syncytia (50, 51), atypical mitotic figures (19, 20), and apoptosis in the absence of vMIA (39, 52). Remarkably, all of these properties can be attributed to a single amino acid residue in gB, resulting in a highly fusogenic gB variant.

Two studies have shown that HCMV enters fibroblasts by envelope fusion with the plasma membrane (41, 42), while another study has reported entry by macropinocytosis (43). Our results demonstrate that a single amino acid residue of gB affects the entry mode of HCMV strain AD169. While AD169 gB(275Y) entered fibroblasts rapidly, AD169 gB(275D) entered more slowly, and this delayed entry was inhibited by the macropinocytosis inhibitor EIPA (Fig. 6). Whether the fast entry mode represents envelope fusion with the plasma membrane as previously reported (41, 42), and whether the delayed entry mode represents macropinocytosis, can only be determined in more extensive studies involving electron microscopy and the use of several different inhibitors. Moreover, it should be noted that gB cooperates with the trimeric gH/gL/gO and the pentameric gH/gL/UL128-131 complexes for entry (53–55). Thus, the increased fusogenicity might either be the result of an inherently hyperfusogenic gB or an altered interaction of gB with other components of the fusion machinery. Moreover, variants of the trimeric and pentameric gH/gL complexes might also affect the mode of entry into fibroblasts. Studies with different HCMV strains will be necessary to determine the requirements for rapid entry by envelope fusion with the plasma membrane. It should also be interesting to determine whether envelope fusion with the plasma membrane inevitably leads to the formation of syncytia with all its potentially deleterious consequences.

The highly fusogenic gB(275Y) variant is present in all sequenced AD169 variants. However, since the original clinical sample that led to the isolation of strain AD169 in 1956 (56) is no longer available, it remains unclear whether the gB(275Y) variant was present in the original virus or arose later during cell culture adaptation. The same is true for the gB(585G) variant of strain VR1814, which has also been passaged many times in cell culture (49). Interestingly, syncytial gB variants have also been described for herpes simplex virus type 1 (57). In most of the analyzed cases, the syncytial gB variants have arisen during cell culture passage, but in 1 case the syncytial phenotype was detected in 2 independent isolates from the same patient (57, 58). Similarly, the presence of the gB(275Y) variant in the clinical HCMV isolate N12 (GenBank accession no. CAA07368) suggests that highly fusogenic gB variants exist in human patients. Moreover, a recent study reported syncytium-forming phenotypes among clinical HCMV isolates from congenitally infected infants (59). This raises the intriguing question of whether syncytium-forming HCMV strains might be associated with increased transmission or pathogenicity. This should be a question worth investigating in future studies.

Materials and Methods

Cells and Viruses. MRC-5 human embryo lung fibroblasts (CCL-171) were obtained from the American Type Culture Collection (ATCC). ATM-deficient

dermal fibroblasts (GM02530) and control cells (GM07532) were purchased from the Coriell Institute. Telomerase-immortalized HFF have been described previously (60). Human embryonic kidney 293A and 293T cells were purchased from Invitrogen and the ATCC, respectively. Phoenix-A, a 293T-derived cell line stably expressing gag, pol, and env for retroviral packaging, have been described previously (61). All cells were grown in DMEM supplemented with 10% FCS, 100 U/mL penicillin and 100 μg/mL streptomycin.

The following HCMV strains were used: AD169-GFP (62), Toledo (63), VR1814 (64), BAC clones of AD169varATCC (65) and AD169varL (66), BAC clones of Towne (67), TB40/E (68), TR, PH (28), and FIX-GFP (69). Reconstitution of infectious HCMV from BAC DNA was done as described previously (31). Viral titers were determined by using the median tissue culture infective dose ($TCID_{50}$) method (70).

Plasmids and Reagents. The pLXSN-mCherry, pLXSN-EGFP and pLXSN-BFP were generated by Gibson cloning using a Gibson Assembly Ultra Kit (VWR). The coding sequence of mCherry, EGFP, and BFP were PCR-amplified from plasmid pmCherry-N1 (Clontech), pEGFP-C1, and pLeGo-iB2/puro-opt (provided by Simon Weißmann, Heinrich Pette Institute, Hamburg, Germany), respectively. The murine leukemia virus-based retroviral plasmid pLXSN (Clontech) was linearized by digestion with enzymes EcoRI and BamHI. The cloning vector pBR322 was a gift from Marion Ziegler, Heinrich Pette Institute, Hamburg, Germany. Plasmids pEPkan-S plasmid (71), pLXSN-HA-E1B19K (72), pSicoR-CRISPR-puroR, pMD2.G, and pCMVR8.91 (73) have been described previously. *Escherichia coli* strain GS1783 (DH10B λcI857Δ(cro-bioA)<>araC-PBADI-sceI) (71) was grown in LB broth (Lennox) containing 5 g/L NaCl (Sigma-Aldrich). Antibiotics were purchased from Roth or Invitrogen and used at the following concentrations: ampicillin (100 μg/mL), kanamycin (50 μg/mL), chloramphenicol (15 μg/mL), and zeocin (25 μg/mL). L-(+)-arabinose was purchased from Sigma-Aldrich. The caspase-8 inhibitor Z-IETD-FMK was purchased from BioCat. The ATM inhibitor KU-60019 was purchased from Selleckchem, the mitosis inhibitors nocodazole and RO-3006 from Sigma, and the macropinocytosis inhibitor EIPA from Santa Cruz.

CRISPR/Cas9 Mutagenesis. Gene knockout cell lines were generated using a previously described CRISPR/Cas9 gene-editing system (73). Guide RNAs for genes of interest were designed using the online tool E-CRISP (http://www.e-crisp.org/E-CRISP/designcrispr.html). The following gRNAs were used to target PIDD (GCTGGCAGCCCCCGGGGTAC [gRNA1]; GAGCTTGGACCTGTACCCCG [gRNA2]; GCGATGGCTGCAACGGTGGA [gRNA3]) and RAIDD (GCAGGAGCATTGTTTTCCGG [gRNA1]; GACCCAGGGAAACTCCTGTA [gRNA2]; GGGCCAGCTGGTTAATCTGC [gRNA3]). They were inserted into the lentiviral vector pSicoR-CRISPR-puroR, and lentiviruses were produced in 293T cells using standard third-generation packaging vectors (73). Lentiviruses were used to transduce HFF cells in the presence of polybrene (5 μg/mL). Cells were selected with 5 μg/mL puromycin (Sigma) and single-cell clones were obtained by limiting dilution.

Mutagenesis of HCMV Genomes. Point mutations were introduced into BAC clones of AD169varL, TB40/E, and FIX-GFP by *en passant* mutagenesis (71). *UL37x1* was deleted as described previously (52). AD169-TB40/E chimeras were constructed using copy-paste mutagenesis as shown in Fig. 4*A* and described in detail elsewhere (31). All modified BACs were examined by restriction fragment analysis and sequencing of the mutated region. The AD169 gB(275D) and TB40/E gB(275Y) BACs were sequence verified by Illumina sequencing essentially as described previously (65). The complete genome sequences of TB40-BAC4 (accession no. EF999921), TR-BAC (accession no. AC146906), FIX-BAC (accession no. AC146907), Towne-BAC (accession no. KF493877), and PH-BAC (accession no. AC146904) are available at GenBank. The complete sequence of AD169*var*L BAC was kindly provided to us by Vu Thuy Khanh Le-Trilling, University Duisburg-Essen, Germany. It is almost identical to the AD169*var*UC sequence (GenBank accession no. FJ527563). The complete genome sequence of Toledo (GU937742) and VR1814 (GU179289) are also available at GenBank.

Immunoblot and Immunofluorescence Analysis. Immunoblot analysis was performed according to standard protocols. Briefly, cells were lysed in SDS sample buffer. Samples were separated by SDS/PAGE and transferred onto nitrocellulose membranes (Amersham) by semidry (for proteins <200 kDa) or wet blotting (for proteins >200 kDa). Proteins of interest were detected with specific primary antibodies and secondary antibodies coupled to horseradish peroxidase (Jackson ImmunoResearch).

Immunofluorescence analysis was performed as previously described (74) with a few modifications. MRC-5 cells were grown on μ-slides (8-well, Ibidi). After treatment or infection, cells were fixed, permeabilized, blocked, and stained with primary antibody overnight at 4 °C and secondary antibodies coupled to AlexaFluor 488 or 555 (Life Technologies). DAPI (Sigma) was used to stain nuclear DNA. Pictures were taken using a Nikon A1+ LSM confocal microscope.

The following primary antibodies were used: γ-tublin (GTU-88, Sigma), β-actin (AC-74, Sigma), caspase-2 (11B4, Millipore), ATM (D2E2, Cell Signaling), caspase-8 (1C12, Cell Signaling), caspase-3 (8G10, Cell Signaling), RAIDD (4B12, MBL), PIDD (Anto-1, Enzo Life Science), HCMV pUL44 (CA006, Virusys), MCP [28-4 (75)], gB [58-15 (76)]. Monoclonal antibodies against HCMV IE1 (1B12), IE1/2 (3H4), pUL36 (10C8), and pp65 (8F5) were a generous gift from Thomas Shenk, Princeton University, Princeton, NJ.

Cell Fusion Assay. MRC-5 fibroblasts expressing mCherry, EGFP, or BFP were generated by transduction with retroviral vectors essentially as described previously (61): Phoenix-A cells were transfected with plasmid pLXSN-mCherry, pLXSN-EGFP or pLXSN-BFP, respectively, and retroviral vectors were used to transduce MRC-5 cells. Transduced cells were selected by 400 μg/mL G418 (Life Technologies). Equal numbers of MRC-5 cells expressing mCherry and EGFP or BFP cells were combined and infected with HCMV. Cells were fixed 48 hpi with 4% PFA, stained with DAPI to visualize nuclei, and analyzed by confocal microscopy.

Cell Cycle Synchronization. MRC-5 fibroblasts were synchronized according to a previously described protocol (77) with a few modifications. To synchronize cells in G0, cells were cultured in serum-free medium for 3 d. To synchronize cells in early G1 (E-G1), cells were cultured in medium containing 0.1% serum for 3 d. E-G1 cells were cultured in medium containing 10% serum for 18 h to synchronize cells in late G1 (L-G1). L-G1 cells were further cultured in medium containing 10% serum for 28 h to push cells into G2. The culture medium was supplemented with 100 ng/mL nocodazole (Sigma) for 20 h to inhibit cells from exiting the M phase. Synchronized cells were collected, fixed with 75% ethanol, stained with propidium iodide (Sigma), and analyzed by flow cytometry.

Cell Viability Assay. MRC-5 cells were infected with HCMV (multiplicity of infection [MOI] 0.1) in a 96-well plate. Cell viability was determined 5 d postinfection (dpi) by measuring intracellular ATP level with a Cell Titer-Glo Luminescent Cell Viability Assay kit (Promega) and a FLUOstar Omega (BMG Labtech) luminometer.

Quantification of HCMV Genomes. Total DNA was extracted from supernatants of HCMV-infected MRC-5 cells using an InnuPREP DNA Mini Kit (Analytik Jena) and subjected to quantitative real-time PCR. Primers ACGCAAAGAGTTCCTCGTAC and TGAACATAACCACGTCCTCG were used to PCR-amplify a piece (*UL36*) of the viral genome. Serial dilutions of the plasmid pcDNA-UL36 were used to generate a standard curve. qPCR was performed by a 7900HT Fast Real-Time PCR System (ThermoFisher Scientific).

Virus Purification. HCMV stocks were produced from supernatants of infected fibroblasts and purified by ultracentrifugation through a sucrose cushion. First, cells and debris were removed by centrifugation at 5,500 × *g* for 15 min. Then the virus was pelleted by centrifugation at 27,000 × *g* for 3 h and resuspended in 2 mL of complete medium. The virus suspension was layered onto a 20% sucrose cushion (18 mL) and centrifuged at 50,126 × *g* for 90 min. The pellet was resuspended in 1 mL of complete medium. Gradient-purified virus stock preparations were obtained by glycerol-tartrate gradient centrifugation (78). Briefly, the virus was pelleted by centrifugation at 27,000 × *g* for 3 h, resuspended in 2 mL of 40 mM Na-phosphate buffer, and carefully loaded onto glycerol-tartrate gradients (4 mL of 35% Na-tartrate and 5 mL of 15% Na-tartrate/30% glycerol) prepared directly before use. Fractionation was done by centrifugation at 90,000 × *g* for 45 min. The virion-containing band was collected with a syringe.

Statistical Analysis. GraphPad Prism 5.0 Software was used to perform statistical analyses. Significance was calculated using 1-way ANOVA with Tukey's multiple comparison post test.

ACKNOWLEDGMENTS. We thank Renke Brixel for technical assistance; the Heinrich Pette Institute technology platforms for BAC sequencing, flow cytometry, and microscopy support; Theodore Potgieter for critical reading of the manuscript; and Andreas Villunger for helpful advice. This research was supported by the Deutsche Forschungsgemeinschaft BR1730/3-2 and BR1730/7-1 [KFO296] (to W.B.). J.T. was supported by a scholarship from the China Scholarship Council.

1. E. S. Mocarski, T. Shenk, P. D. Griffiths, R. F. Pass, "Cytomegaloviruses" in *Fields Virology*, D. M. Knipe, P. M. Howley, Eds. (Lippincott, Williams & Wilkins, Philadelphia), ed. 6, 2013), pp. 1960–2014.
2. C. S. Cobbs *et al*., Human cytomegalovirus infection and expression in human malignant glioma. *Cancer Res.* **62**, 3347–3350 (2002).
3. G. Herbein, The human cytomegalovirus, from oncomodulation to oncogenesis. *Viruses* **10**, e408 (2018).
4. R. F. Kalejta, T. Shenk, Manipulation of the cell cycle by human cytomegalovirus. *Front. Biosci.* **7**, d295–d306 (2002).
5. D. H. Spector, Human cytomegalovirus riding the cell cycle. *Med. Microbiol. Immunol.* **204**, 409–419 (2015).
6. H. Weisbach *et al*., Synthetic lethal mutations in the cyclin A interface of human cytomegalovirus. *PLoS Pathog.* **13**, e1006193 (2017).
7. E. Xiaofei, T. F. Kowalik, The DNA damage response induced by infection with human cytomegalovirus and other viruses. *Viruses* **6**, 2155–2185 (2014).
8. J. P. Castillo *et al*., Human cytomegalovirus IE1-72 activates ataxia telangiectasia mutated kinase and a p53/p21-mediated growth arrest response. *J. Virol.* **79**, 11467–11475 (2005).
9. M. Gaspar, T. Shenk, Human cytomegalovirus inhibits a DNA damage response by mislocalizing checkpoint proteins. *Proc. Natl. Acad. Sci. U.S.A.* **103**, 2821–2826 (2006).
10. M. H. Luo, K. Rosenke, K. Czornak, E. A. Fortunato, Human cytomegalovirus disrupts both ataxia telangiectasia mutated protein (ATM)- and ATM-Rad3-related kinase-mediated DNA damage responses during lytic infection. *J. Virol.* **81**, 1934–1950 (2007).
11. A. Ciccia, S. J. Elledge, The DNA damage response: Making it safe to play with knives. *Mol. Cell* **40**, 179–204 (2010).
12. W. Brune, C. E. Andoniou, Die another day: Inhibition of cell death pathways by cytomegalovirus. *Viruses* **9**, E249 (2017).
13. V. S. Goldmacher *et al*., A cytomegalovirus-encoded mitochondria-localized inhibitor of apoptosis structurally unrelated to Bcl-2. *Proc. Natl. Acad. Sci. U.S.A.* **96**, 12536–12541 (1999).
14. A. Skaletskaya *et al*., A cytomegalovirus-encoded inhibitor of apoptosis that suppresses caspase-8 activation. *Proc. Natl. Acad. Sci. U.S.A.* **98**, 7829–7834 (2001).
15. S. Kumar, Caspase 2 in apoptosis, the DNA damage response and tumour suppression: Enigma no more? *Nat. Rev. Cancer* **9**, 897–903 (2009).
16. J. Forsberg, B. Zhivotovsky, M. Olsson, Caspase-2: An orphan enzyme out of the shadows. *Oncogene* **36**, 5441–5444 (2017).
17. A. Tinel, J. Tschopp, The PIDDosome, a protein complex implicated in activation of caspase-2 in response to genotoxic stress. *Science* **304**, 843–846 (2004).
18. K. Ando *et al*., PIDD death-domain phosphorylation by ATM controls prodeath versus prosurvival PIDDosome signaling. *Mol. Cell* **47**, 681–693 (2012).
19. L. Hertel, E. S. Mocarski, Global analysis of host cell gene expression late during cytomegalovirus infection reveals extensive dysregulation of cell cycle gene expression and induction of Pseudomitosis independent of US28 function. *J. Virol.* **78**, 11988–12011 (2004).
20. L. Hertel, S. Chou, E. S. Mocarski, Viral and cell cycle-regulated kinases in cytomegalovirus-induced pseudomitosis and replication. *PLoS Pathog.* **3**, e6 (2007).
21. A. L. Vanarsdall, D. C. Johnson, Human cytomegalovirus entry into cells. *Curr. Opin. Virol.* **2**, 37–42 (2012).
22. R. Thompson *et al*., An inhibitor of PIDDosome formation. *Mol. Cell* **58**, 767–779 (2015).
23. L. L. Fava *et al*., The PIDDosome activates p53 in response to supernumerary centrosomes. *Genes Dev.* **31**, 34–45 (2017).
24. S. Dawar *et al*., Caspase-2-mediated cell death is required for deleting aneuploid cells. *Oncogene* **36**, 2704–2714 (2017).
25. E. A. Fortunato, V. Sanchez, J. Y. Yen, D. H. Spector, Infection of cells with human cytomegalovirus during S phase results in a blockade to immediate-early gene expression that can be overcome by inhibition of the proteasome. *J. Virol.* **76**, 5369–5379 (2002).
26. M. Zydek, C. Hagemeier, L. Wiebusch, Cyclin-dependent kinase activity controls the onset of the HCMV lytic cycle. *PLoS Pathog.* **6**, e1001096 (2010).
27. L. L. Fava, F. J. Bock, S. Geley, A. Villunger, Caspase-2 at a glance. *J. Cell Sci.* **125**, 5911–5915 (2012).
28. E. Murphy *et al*., Coding potential of laboratory and clinical strains of human cytomegalovirus. *Proc. Natl. Acad. Sci. U.S.A.* **100**, 14976–14981 (2003).
29. N. Renzette, B. Bhattacharjee, J. D. Jensen, L. Gibson, T. F. Kowalik, Extensive genome-wide variability of human cytomegalovirus in congenitally infected infants. *PLoS Pathog.* **7**, e1001344 (2011).
30. H. Costa, R. Nascimento, J. Sinclair, R. M. Parkhouse, Human cytomegalovirus gene UL76 induces IL-8 expression through activation of the DNA damage response. *PLoS Pathog.* **9**, e1003609 (2013).
31. J. Tang, R. Brixel, W. Brune, *Copy-paste* mutagenesis: A method for large-scale alteration of viral genomes. *Int. J. Mol. Sci.* **20**, e913 (2019).
32. D. Yu, M. C. Silva, T. Shenk, Functional map of human cytomegalovirus AD169 defined by global mutational analysis. *Proc. Natl. Acad. Sci. U.S.A.* **100**, 12396–12401 (2003).
33. E. M. Borst, K. Wagner, A. Binz, B. Sodeik, M. Messerle, The essential human cytomegalovirus gene UL52 is required for cleavage-packaging of the viral genome. *J. Virol.* **82**, 2065–2078 (2008).
34. D. Navarro *et al*., Glycoprotein B of human cytomegalovirus promotes virion penetration into cells, transmission of infection from cell to cell, and fusion of infected cells. *Virology* **197**, 143–158 (1993).
35. M. K. Isaacson, T. Compton, Human cytomegalovirus glycoprotein B is required for virus entry and cell-to-cell spread but not for virion attachment, assembly, or egress. *J. Virol.* **83**, 3891–3903 (2009).
36. P. T. Wille, T. W. Wisner, B. Ryckman, D. C. Johnson, Human cytomegalovirus (HCMV) glycoprotein gB promotes virus entry in trans acting as the viral fusion protein rather than as a receptor-binding protein. *MBio* **4**, e00332-13 (2013).
37. S. Tugizov *et al*., Function of human cytomegalovirus glycoprotein B: Syncytium formation in cells constitutively expressing gB is blocked by virus-neutralizing antibodies. *Virology* **201**, 263–276 (1994).
38. Z. Storchova, C. Kuffer, The consequences of tetraploidy and aneuploidy. *J. Cell Sci.* **121**, 3859–3866 (2008).
39. M. Reboredo, R. F. Greaves, G. Hahn, Human cytomegalovirus proteins encoded by UL37 exon 1 protect infected fibroblasts against virus-induced apoptosis and are required for efficient virus replication. *J. Gen. Virol.* **85**, 3555–3567 (2004).
40. A. L. McCormick, C. D. Meiering, G. B. Smith, E. S. Mocarski, Mitochondrial cell death suppressors carried by human and murine cytomegalovirus confer resistance to proteasome inhibitor-induced apoptosis. *J. Virol.* **79**, 12205–12217 (2005).
41. J. D. Smith, E. de Harven, Herpes simplex virus and human cytomegalovirus replication in WI-38 cells. II. An ultrastructural study of viral penetration. *J. Virol.* **14**, 945–956 (1974).
42. T. Compton, R. R. Nepomuceno, D. M. Nowlin, Human cytomegalovirus penetrates host cells by pH-independent fusion at the cell surface. *Virology* **191**, 387–395 (1992).
43. S. Hetzenecker, A. Helenius, M. A. Krzyzaniak, HCMV induces macropinocytosis for host cell entry in fibroblasts. *Traffic* **17**, 351–368 (2016).
44. B. Bodaghi *et al*., Entry of human cytomegalovirus into retinal pigment epithelial and endothelial cells by endocytosis. *Invest. Ophthalmol. Vis. Sci.* **40**, 2598–2607 (1999).
45. B. J. Ryckman, M. A. Jarvis, D. D. Drummond, J. A. Nelson, D. C. Johnson, Human cytomegalovirus entry into epithelial and endothelial cells depends on genes UL128 to UL150 and occurs by endocytosis and low-pH fusion. *J. Virol.* **80**, 710–722 (2006).
46. A. L. Vanarsdall, T. W. Wisner, H. Lei, A. Kazlauskas, D. C. Johnson, PDGF receptor-α does not promote HCMV entry into epithelial and endothelial cells but increased quantities stimulate entry by an abnormal pathway. *PLoS Pathog.* **8**, e1002905 (2012).
47. G. Gerna, E. Percivalle, L. Perez, A. Lanzavecchia, D. Lilleri, Monoclonal antibodies to different components of the human cytomegalovirus (HCMV) pentamer gH/gL/pUL128L and trimer gH/gL/gO as well as antibodies elicited during primary HCMV infection prevent epithelial cell syncytium formation. *J. Virol.* **90**, 6216–6223 (2016).
48. G. Hahn *et al*., The human cytomegalovirus ribonucleotide reductase homolog UL45 is dispensable for growth in endothelial cells, as determined by a BAC-cloned clinical isolate of human cytomegalovirus with preserved wild-type characteristics. *J. Virol.* **76**, 9551–9555 (2002).
49. D. J. Dargan *et al*., Sequential mutations associated with adaptation of human cytomegalovirus to growth in cell culture. *J. Gen. Virol.* **91**, 1535–1546 (2010).
50. V. Vonka, E. Anisimová, M. Macek, Replication of cytomegalovirus in human epitheloid diploid cell line. *Arch. Virol.* **52**, 283–296 (1976).
51. D. Wang, T. Shenk, Human cytomegalovirus UL131 open reading frame is required for epithelial cell tropism. *J. Virol.* **79**, 10330–10338 (2005).
52. W. Brune, M. Nevels, T. Shenk, Murine cytomegalovirus m41 open reading frame encodes a Golgi-localized antiapoptotic protein. *J. Virol.* **77**, 11633–11643 (2003).
53. A. L. Vanarsdall, P. W. Howard, T. W. Wisner, D. C. Johnson, Human cytomegalovirus gH/gL forms a stable complex with the fusion protein gB in virions. *PLoS Pathog.* **12**, e1005564 (2016).
54. A. L. Vanarsdall, B. J. Ryckman, M. C. Chase, D. C. Johnson, Human cytomegalovirus glycoproteins gB and gH/gL mediate epithelial cell-cell fusion when expressed either in cis or in trans. *J. Virol.* **82**, 11837–11850 (2008).
55. M. Zhou, J. M. Lanchy, B. J. Ryckman, Human cytomegalovirus gH/gL/gO promotes the fusion step of entry into all cell types, whereas gH/gL/UL128-131 broadens virus tropism through a distinct mechanism. *J. Virol.* **89**, 8999–9009 (2015).
56. W. P. Rowe, J. W. Hartley, S. Waterman, H. C. Turner, R. J. Huebner, Cytopathogenic agent resembling human salivary gland virus recovered from tissue cultures of human adenoids. *Proc. Soc. Exp. Biol. Med.* **92**, 418–424 (1956).
57. L. R. Parsons *et al*., Rapid genome assembly and comparison decode intrastrain variation in human alphaherpesviruses. *MBio* **6**, e02213-14 (2015).
58. M. Heller, R. D. Dix, J. R. Baringer, J. Schachter, J. E. Conte Jr, Herpetic proctitis and meningitis: Recovery of two strains of herpes simplex virus type 1 from cerebrospinal fluid. *J. Infect. Dis.* **146**, 584–588 (1982).
59. G. Galitska *et al*., Biological relevance of cytomegalovirus genetic variability in congenitally and postnatally infected children. *J. Clin. Virol.* **108**, 132–140 (2018).
60. W. A. Bresnahan, G. E. Hultman, T. Shenk, Replication of wild-type and mutant human cytomegalovirus in life-extended human diploid fibroblasts. *J. Virol.* **74**, 10816–10818 (2000).
61. S. Swift, J. Lorens, P. Achacoso, G. P. Nolan, (2001) Rapid production of retroviruses for efficient gene delivery to mammalian cells using 293T cell-based systems. *Curr. Protoc. Immunol.* **Chapter 10**, Unit 10.17C.
62. M. Marschall, M. Freitag, S. Weiler, G. Sorg, T. Stamminger, Recombinant green fluorescent protein-expressing human cytomegalovirus as a tool for screening antiviral agents. *Antimicrob. Agents Chemother.* **44**, 1588–1597 (2000).
63. J. M. Brown, H. Kaneshima, E. S. Mocarski, Dramatic interstrain differences in the replication of human cytomegalovirus in SCID-hu mice. *J. Infect. Dis.* **171**, 1599–1603 (1995).
64. M. Grazia Revello *et al*., In vitro selection of human cytomegalovirus variants unable to transfer virus and virus products from infected cells to polymorphonuclear leukocytes and to grow in endothelial cells. *J. Gen. Virol.* **82**, 1429–1438 (2001).
65. E. Ostermann, M. Spohn, D. Indenbirken, W. Brune, Complete genome sequence of a human cytomegalovirus strain AD169 bacterial artificial chromosome clone. *Genome Announc.* **4**, e00091-16 (2016).

66. V. T. Le, M. Trilling, H. Hengel, The cytomegaloviral protein pUL138 acts as potentiator of tumor necrosis factor (TNF) receptor 1 surface density to enhance ULb'-encoded modulation of TNF-α signaling. *J. Virol.* **85**, 13260–13270 (2011).
67. A. Marchini, H. Liu, H. Zhu, Human cytomegalovirus with IE-2 (UL122) deleted fails to express early lytic genes. *J. Virol.* **75**, 1870–1878 (2001).
68. C. Sinzger *et al*., Cloning and sequencing of a highly productive, endotheliotropic virus strain derived from human cytomegalovirus TB40/E. *J. Gen. Virol.* **89**, 359–368 (2008).
69. F. Goodrum, M. Reeves, J. Sinclair, K. High, T. Shenk, Human cytomegalovirus sequences expressed in latently infected individuals promote a latent infection in vitro. *Blood* **110**, 937–945 (2007).
70. J. C. Hierholzer, R. A. Killington, "Virus isolation and quantitation" in *Virology Methods Manual*, H. Kangro, B. Mahy, Eds. (Academic Press, San Diego, 1996).
71. B. K. Tischer, G. A. Smith, N. Osterrieder, En passant mutagenesis: A two step markerless red recombination system. *Methods Mol. Biol.* **634**, 421–430 (2010).
72. I. Jurak, W. Brune, Induction of apoptosis limits cytomegalovirus cross-species infection. *EMBO J.* **25**, 2634–2642 (2006).
73. F. R. van Diemen *et al*., CRISPR/Cas9-Mediated genome editing of herpesviruses limits productive and latent infections. *PLoS Pathog.* **12**, e1005701 (2016).
74. T. Schommartz, J. Tang, R. Brost, W. Brune, Differential requirement of human cytomegalovirus UL112-113 protein isoforms for viral replication. *J. Virol.* **91**, e00254-17 (2017).
75. V. Sanchez, K. D. Greis, E. Sztul, W. J. Britt, Accumulation of virion tegument and envelope proteins in a stable cytoplasmic compartment during human cytomegalovirus replication: Characterization of a potential site of virus assembly. *J. Virol.* **74**, 975–986 (2000).
76. W. J. Britt, L. G. Vugler, Oligomerization of the human cytomegalovirus major envelope glycoprotein complex gB (gp55-116). *J. Virol.* **66**, 6747–6754 (1992).
77. L. Wiebusch, A. Neuwirth, L. Grabenhenrich, S. Voigt, C. Hagemeier, Cell cycle-independent expression of immediate-early gene 3 results in G1 and G2 arrest in murine cytomegalovirus-infected cells. *J. Virol.* **82**, 10188–10198 (2008).
78. S. Reyda, N. Büscher, S. Tenzer, B. Plachter, Proteomic analyses of human cytomegalovirus strain AD169 derivatives reveal highly conserved patterns of viral and cellular proteins in infected fibroblasts. *Viruses* **6**, 172–188 (2014).